
DEEP MULTI-SHOT NETWORK FOR MODELLING APPEARANCE SIMILARITY IN MULTI-PERSON TRACKING APPLICATIONS

M. J. Gómez-Silva
Intelligent Systems Lab (LSI) Research Group,
Universidad Carlos III de Madrid,
Leganés, Madrid, Spain
magomezs@ing.uc3m.es

April 8, 2020

ABSTRACT

The automatization of Multi-Object Tracking becomes a demanding task in real unconstrained scenarios, where the algorithms have to deal with crowds, crossing people, occlusions, disappearances and the presence of visually similar individuals. In those circumstances, the data association between the incoming detections and their corresponding identities could miss some tracks or produce identity switches. In order to reduce these tracking errors, and even their propagation in further frames, this article presents a Deep Multi-Shot neural model for measuring the Degree of Appearance Similarity (MS-DoAS) between person observations. This model provides temporal consistency to the individuals' appearance representation, and provides an affinity metric to perform frame-by-frame data association, allowing online tracking. The model has been deliberately trained to be able to manage the presence of previous identity switches and missed observations in the handled tracks. With that purpose, a novel data generation tool has been designed to create training tracklets that simulate such situations. The model has demonstrated a high capacity to discern when a new observation corresponds to a certain track, achieving a classification accuracy of 97% in a hard test that simulates tracks with previous mistakes. Moreover, the tracking efficiency of the model in a Surveillance application has been demonstrated by integrating that into the frame-by-frame association of a Tracking-by-Detection algorithm.

Keywords Deep Neural Network · Appearance Similarity · Multi-Shot Recognition · Multi-Object Tracking

1 Introduction

Multi-Object Tracking (MOT) task consists of visually finding the location of multiple individuals from their visual measurements and conserving their identities in an image sequence.

In the context of Intelligent Surveillance Systems, the automatization of the MOT task is essential to manage the huge amount of data captured from a large-scale distributed network of cooperative sensors and consequently, to automatically monitor multiple individuals in wide areas. This automatization relies on the proper association between the consecutive observations of each individual along a surveillance sequence.

In real unconstrained and crowded scenarios, the tracking of multiple individuals is hampered by a wide variety of challenging situations: fast-moving people or moving camera platforms, presence of crowds, crossing people, people with changing-trajectories, partially or total occlusions along short or long term, people disappearing from the monitored area, or new individuals entering in the field of view of the surveillance camera.

The performance of the data association process substantially depends on the design of the person representation and on the formulation of the cost function. This function is a metric to measure the cost of assigning a certain identity to a certain detection. Consequently, data association methods based on only motion cues or targets' dynamics, e.g. [1], are not able to handle agents with varying trajectories. This circumstance boosts the research on modelling individuals' appearance to improve the performance of online methods.

In addition, no information about the agents appearing in the scene is known in advance. Given the unpredictable nature of the surveillance task, an essential capacity for MOT algorithms is the versatility to be applied to any unknown individual, who must be recognised among a high number of observations.

To achieve that, instead of learning a number of specified patterns for each one of the tracked agents, e.g. [2], this article proposes the design of a unique deep neural model. The proposed network jointly models the appearance features of multiple person detections and an affinity metric to compare them, which results in the measurement of the Degree of Appearance Similarity (DoAS) between the person images. This model identifies the affinity between different images of the same person, allowing the tracking of multiple people using the same model for all of them. In that way, unlike online-learning models approaches, the developed method does not require previous knowledge about the scene and neither a large number of frames to learn a robust model for an agent's appearance.

The recognition of a person by means of an appearance neural model presents an intrinsically unbalanced nature, given the lack of data about the people to identify and the huge number of possible false assignments with surrounding agents. This results in the collapse and over-fitting of the neural model. For that reason, a novel formulation to generate the proper training data to feed the model is proposed in this work.

Once the model is trained and integrated into a data association process, its performance in complex scenes could produce some identities switches, i.e. the association of incorrect identities to some detections. After an identity switch, a different person's track is associated with an agent in further iterations, making very difficult the correction of such error.

With the aim of avoiding identity switches or dealing with the consequences of a previous mismatching, and in order to avoid the error propagation in further frames, temporal consistency has been implicitly added to the model through a novel contrastive network architecture design. This follows a Multi-Shot recognition approach, whose core is a Long Short Term Memory (LSTM) cell.

A Deep Convolutional Neural Network has been modelled to render the appearance of the individuals through a feature array. The obtained features for a certain individual at different frames are related by the LSTM cell, providing the global appearance feature for a certain track. This is compared with the new observations by the proposed model. The result is a contrastive metric, hereinafter called Multi-Shot DoAS. In that way, every detection is compared by a model that considers not only the last saved observations but also those from previous frames.

Therefore, this article presents a novel neural model to measure the Multi-Shot Degree of Appearance Similarity (MS-DoAS) between person images to perform the association of individuals' observations through different frames in a Multi-Object Tracking algorithm. The main contributions of the proposed method are:

- i. Design of a novel Deep Neural Network architecture for performing Multi-Shot recognition of any unknown individual. This model relies on the temporal consistency of the agent's appearance by analysing the visual features measured in previous frames.
- ii. Formulation of a training process that makes the model able to face complex real surveillance situations, including short-term disappearances of the agents, missed detections, and occlusions. Moreover, the resultant model is also able to deal with previously failed associations, preventing from further propagation of the identities mismatching. These capabilities have been acquired by training it on a variate set of tracklets (fragments of tracks), especially generated with such purpose by deliberately introducing temporal steps between some captures, as well as, intruder detections¹.
- iii. Integration of the proposed model in the data association process of an online Multi-Object Tracking algorithm. The affinity measure given by the proposed model, MS-DoAS, has been used, together with other motion cues, as part of a multi-modal cost function.

The proposed model provides temporary consistency by modelling the agents' appearance with an LSTM network which is fed by features from previous frames. In that way, the propagation of punctual association mistakes is avoided, without requiring extending the association process through multiple future frames, as batch methods do. Hence, the proposed model allows an online tracking algorithm, with a frame-to-frame assignment.

The effectiveness of the proposed model has been proved by measuring its recognition capacity over multiple and variate test sets, and also by evaluating the final performance of an MOT algorithm where the model is integrated.

The rest of the article is structured as follows: the second Section presents a review of the existing related works. Section 3 describes the proposed Re-Id neural model, and Section 4 the developed learning algorithm to train it. Finally, Section 5 and 6 present the obtained experimental results and some concluding remarks, respectively.

¹The tracklets generation tool has been implemented as a set of C++ functions, which are publicly available under http://github.com/magomez/dataset_factory/tree/master/data_factory_from_mot

2 Related Work

Although Multi-Object Tracking (MOT) methods have been reviewed intensively, [3], it remains a challenging problem under development. MOT has become a branch of research deeply studied by the scientific community due to its prominent application to Intelligent Surveillance Systems, ISS, since many other applications, such as behaviour analysis, rely on the tracking performance.

Furthermore, Multi-Object Tracking in video sequences is also widely used in other military and civil applications, such as sports players tracking and analysis [4], biology [5], robot navigation [6], and autonomous driving vehicles [7].

In the literature, tracking problem is commonly solved by selecting a detector and feeding a tracker with it, resulting in a wide range of approaches, which have long been encompassed under the paradigm called “tracking-by-detection”.

Once a set of reliable detections is collected, the task of the tracker translates into a data association problem for determining the correspondence of detections across frames. Therefore, the data association consists of finding the correct assignment between the detections at every new frame and their corresponding identities. Identity is given to every trajectory that describes the path of an individual instance over time, hereinafter called agent.

Data association methods are mainly composed of a cost function, which measures the cost of assigning a certain identity to a detected person, and an optimization algorithm, which is in charge of seeking the assignment that minimizes the cost function. Therefore, independently from the association mechanism, a significant part of the final Multi-person tracking performance relies on the proper formulation of the cost metric, whose is limited, in turn, by the person representation design.

Some of the most commonly used features are related to individuals’ motion, such as location, or velocity, and even the interactions between agents. Trajectories have been typically treated as state-space models, like in Kalman [8] or particle filters [9]. Moreover, in [10, 11], trajectories are clustered as a mean to learn motion patterns. Furthermore, another approach is to develop more complex motion models to better predict future trajectories. For instance, Fan et al. [12] used Deep Convolutional Neural Networks (DCNN) to predict the location and scale of an individual for tracking.

However, in crowded scenes, a location or motion-based online association method could find problems to deal with changing-trajectory and crossing agents. There is a vast number of works that exploit appearance information to solve data association and to overcome the dependency on the motion cues. In those cases, a primary task in people tracking is converting raw pixels into higher-level representations.

Some simple appearance models are based on extracting appearance information from the object pixels using hand-crafted features, including colour histogram [13, 14] and texture descriptors [15, 16].

Other approaches use covariance matrix representation, pixel comparison representation and SIFT-like features, or pose features [17]. For instance, in [18] an edgelet-based part model for describing the appearance of objects is presented.

Recently, Deep Convolutional Neural Networks have been used for modelling appearance by learning high-level features, e.g. [19, 20, 21]. For example, in [22] the feature extraction is directly learnt by using a convolutional pipeline that can be completely trained on a vast number of samples.

Other tracking algorithms get improvements by means of modelling every tracked agent independently, e.g. [11, 2]. Since there is no previous knowledge about the people to track, the dedicated models are trained online. The drawback of these approaches is that a certain time is needed until the online learning catches enough number of samples of a person to learn a reliable pattern.

On the other hand, many works explicitly learn affinity or similarity metrics from data, in order to compare two observations, e.g. [20]. These works are characterised by the use of a cost metric in their tracking formulation once the metric has been learnt, but they do not consider the actual inference model during the learning phase.

The recent trend in Multi-Target tracking is the integration of the people features learning into the association scheme method. This approach is applicable to batch association methods, a.k.a. offline methods, such as multi-dimensional alignment algorithms [23] and network flow-based methods [24]. Batch association methods provide temporal context through sets of future observations, allowing for robust predictions.

For example, Multi Hypothesis Tracking method can be extended to include online learned discriminative appearance models for each track hypothesis [22]. On the other hand, in [24], features for Network Flow-based data association are learnt via back-propagation, by expressing the optimum of a smoothed network Flow problem as a differentiable function of the pairwise association costs.

Furthermore, many of the research efforts focused on reducing the tracking errors, exploit the temporal consistency by the extraction of people tracklets, i.e. short object tracks. Unfortunately, the availability of reliable tracklets cannot be guaranteed due to the propagation of mistakes. This effect is pronounced in network flow-based association methods due to their limited

capacity to model complex appearance changes. An alternative is to define pairwise costs between tracklets that can be reliably computed, [25].

In tracklet association, discriminative appearance models are trained with the aim of learning an improved affinity score function, e.g. [10, 26]. However, these are batch methods, which perform multi-frame generalization using tracklets or even the whole sequence at once and on a hierarchical global data association [27], where all the detections are gradually connected after these have been collected for a huge set of frames. Therefore, batch methods rely on future observations and for that reason, they are not applicable in real-time vision systems, where a frame-by-frame association, called online association, is needed.

On the contrary, other methods add temporary consistency to the data association process by using Long Short-Term Memory (LSTM) models. Subsequently, the pairwise terms, which relate two observations, can be weighted by offline trained appearance templates [28] or a simple distance metric between appearance features [27]. For instance, in [29] an LSTM model which learns to predict similar motion and appearance patterns is presented.

Modelling appearance with LSTM cells in an offline learning process and using the obtained models into an online data association method brings together the advantages of allowing a real-time algorithm with temporal consistency, as the work presented in this article demonstrates. This approach does not require any knowledge about individuals and neither time to adapt the model to them, and any unknown agent can be tracked.

3 Degree of Appearance Similarity Model

With the aim of exploiting the visual appearance of a target individual to track him/her among multiple people, an appearance affinity model has been developed.

The differences in visual appearance between a certain agent (tracked identity) and a detection is taken as an affinity cue in their matching cost formulation. Instead of modelling a specific individual’s appearance pattern, a universal model has been designed to predicts whether the images correspond to the same person or not.

Therefore, a comparative metric has been trained to measure the Degree of Appearance Similarity (DoAS) between captures. This has been formulated as a pair-wise binary classification problem to discriminate between groups of images belonging to the same person, or corresponding to different people, which are called positive and negative tracklets, respectively.

3.1 Multi-Shot DoAS Architecture

The Multi-Shot DoAS model, MS-DoAS, measure the appearance affinity between a certain detection, d_i , and a certain agent a_i , and its computation is rendered by the scheme in Fig. 1.

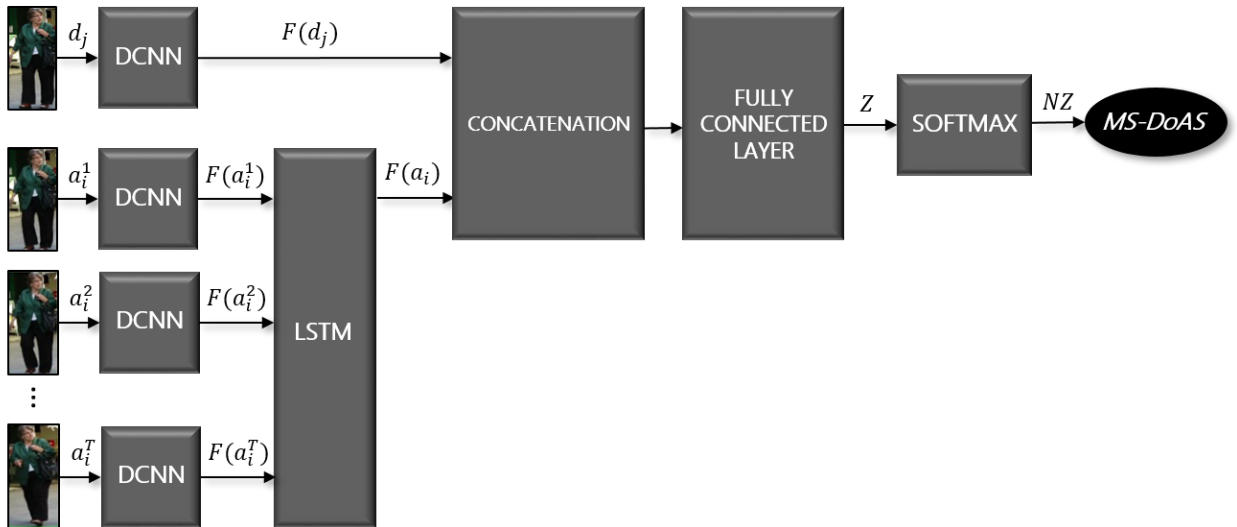


Figure 1: Computation of Multi-Shot Degree of Appearance Similarity, MS-DoAS, between a detection, d_i , and an agent, a_i .

This model follows a multi-shot recognition scheme since a certain detection, captured in the current frame, f , is compared with the visual appearance of a certain agent, not only in the previous iteration, $f - 1$, but in T previously captured images. This Multi-Shot recognition approach provides temporary consistency to obtain an accurate prediction.

Due to certain occlusions, or temporary disappearances, a certain agent could not be detected in consecutive frames. The available captures feed the model in inverse order of acquisition. So, the number, f_1 , of the frame where the representation a_i^t of the agent was acquired is always higher than the number, f_2 , of the frame where the next representation $a_i^{(t+1)}$ was captured, $f_1 > f_2$. Moreover, all these frames are previous to that where the compared detection was found.

The MS-DoAS metric has been computed by modelling the appearance of each compared individual in a feature array. The appearance of the query detection is rendered by a feature array, $F(d_j)$, computed by a pre-trained DCNN.

Analogously, the appearance of each one of the T previously acquired representations of the query agent, a_i^t , is rendered by a feature array, $F(a_i^t)$, previously computed by the same pre-trained DCNN in the frame where it was captured. The saved features about the agent are used as the inputs of a pre-trained Long-Short-Term-Memory (LSTM) cell, which provides a general feature for the agent, $F(a_i)$.

Subsequently, a second group of neural layers are used to model the affinity cue that contrasts the individuals' appearance features. Firstly, $F(d_j)$ and $F(a_i)$ are concatenated to feed a fully connected (FC) layer, which has been also pre-trained. This FC layer is used as a binary classification function, which performs the optimal weighting of the elements of the features $F(d_j)$ and $F(a_i)$ and returns a pair of outputs ($K = 2$) whose values, (Z_0, Z_1) , are representative of the dissimilarity and similarity classes. Finally, a Softmax function, σ , defined by Eq. 1, normalises these values in the range $[0, 1]$.

$$NZ_n = \sigma(Z_n) = \frac{e^{Z_n}}{\sum_{k=0}^{K-1} e^{Z_k}}, \forall n \in [0, 1] \in \mathbb{Z} \quad (1)$$

Due to the contrastive essence of this pair-wise approach, the first normalised output, NZ_0 , returns the probability of that the agent, a_i , and the measurement, d_j , do not form a correct match, and the second, NZ_1 , the probability that they form a correct match. Therefore, NZ_1 is taken as the MS-DoAS between the agent, a_i , and the detection, d_j .

3.2 Features computation

Instead of directly compare the raw images, the comparison is performed from their representative feature arrays. Therefore, it is necessary to model an embedding, $F(I)$, to map an input image, I , to a feature space, such that the distance between samples rendering the same person is smaller than that between different people in that feature space.

In order to deal with partial-term occlusions, after which the representation of a person changes, deep learning has been used to automatically find the most salient features of the individuals' appearance. Hence, the feature embedding has been modelled by a Deep Convolutional Neural Network (DCNN). Therefore, the feature representation for an image, $F_W(I)$, is given by the output of the DCNN, which depends on its weights values, W .

Concretely, the used DCNN model follows an adapted version of the VGG11 architecture, presented as the A version of a set of Very Deep CNNs in [30]. The layers specifications of the proposed VGG11-based embedding are listed in Table 1.

Table 1: Structure of the used VGG11-based model. The input and output sizes are described in $\#rows \times \#cols \times \#filters$; the kernel, in $\#rows \times \#cols \times \#filters, stride$, or $\#outputs$ for FC layers.

Layer	Input size	Output size	Kernel
Conv-1-1	128 x 64 x 3	128 x 64 x 64	3 x 3 x 3
Pool-1	128 x 64 x 64	64 x 32 x 64	2 x 2 x 64, 2
Conv-2-1	64 x 32 x 64	64 x 32 x 128	3 x 3 x 64
Pool-2	64 x 32 x 128	32 x 16 x 128	2 x 2 x 128, 2
Conv-3-1	32 x 16 x 128	32 x 16 x 256	3 x 3 x 128
Conv-3-2	32 x 16 x 256	32 x 16 x 256	3 x 3 x 256
Pool-3	32 x 16 x 256	16 x 8 x 256	2 x 2 x 256, 2
Conv-4-1	16 x 8 x 256	16 x 8 x 512	3 x 3 x 256
Conv-4-2	16 x 8 x 512	16 x 8 x 512	3 x 3 x 512
Pool-4	16 x 8 x 512	8 x 4 x 512	2 x 2 x 512, 2
Conv-5-1	8 x 4 x 512	8 x 4 x 512	3 x 3 x 512
Conv-5-2	8 x 4 x 512	8 x 4 x 512	3 x 3 x 512
Pool-5	8 x 4 x 512	4 x 2 x 512	2 x 2 x 512, 2
FC-6	4 x 2 x 512	1 x 1 x 4096	4096
FC-7	1 x 1 x 4096	1 x 1 x 4096	4096
FC-8	1 x 1 x 4096	1 x 1 x 1000	1000

VGG11 presents eight convolutional layers, three fully connected layers and a SoftMax final layer. The SoftMax layer has been removed to get a feature array as output instead of a classification probability value. Hence, its output is a point in the feature space represented by a 1000-dimensional array $F(I) \in \mathbb{R}^n$ ($n = 1000$). Moreover, the input size used in [30] has been modified to adapt its value to the person detections proportions. Therefore, the input of the proposed DCNN is an RGB image of a fixed size, which has been set 64x128 pixels. All hidden layers are provided of a Rectified Liner Unit, ReLU, [31], as activation function.

This neural network has been trained following the Siamese model, which can perform the discrimination of the pairs of samples in two well-differentiated groups, positive and negative pairs. This discrimination has been accentuated by the use of the Normalised Double-Margin-based Contrastive Loss Function², formulated in [32].

The Pair-based Mini-Batch Gradient Descent Learning Algorithm, presented in [33], has been conducted to learn the network weights. The training data has been generated from the MOT17 dataset of surveillance sequences. A data generation tool was used to extract people detections from the sequences, and subsequently, the detections are combined to create a huge number of training pairs, by means of using the balancing data method³, presented in [33].

Once the neural network was trained, this was used to compute the appearance feature of a person's image⁴.

4 Learning Algorithm

The training architecture used to learn the parameters of the LSTM cell and the FC layer that allow measuring the MS-DoAS is rendered in Fig. 2.

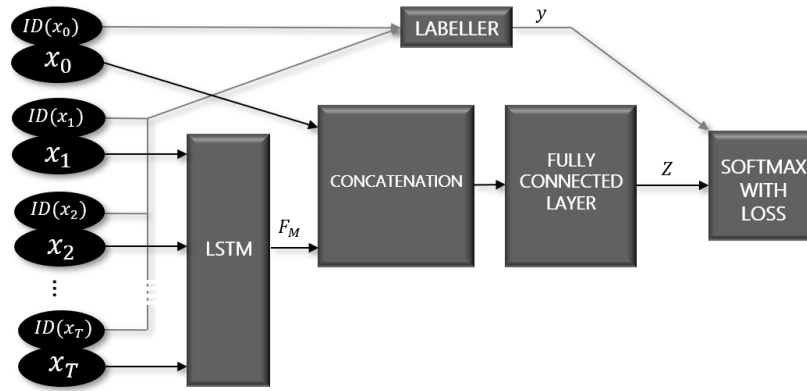


Figure 2: MS-DoAS learning architecture.

Each training sample, $X_i = (x_0, \dots, x_T)$ is formed by an array (with zero-based indexing) of features, called feature tracklet, whose size is $T + 1$, where T is the size of the memory of the LSTM cell. Each tracklet element, x_n , corresponds to a feature computed from an image that was taken from a frame whose number is given by $f(x_n)$.

By computing the features in an offline process, previous to the learning, the training time is highly reduced. The number of possible training tracklets created from a given set of images is much larger than the size of that set of images. For that reason, computing the features of all the images of the set before forming tracklets combinations is much more efficient, as long as the computational time is concerned.

Because the neural model is learnt by a supervised training process, every feature of a tracklet is accompanied by the identification number of the person that it is rendering, $ID(x_n)$. A tracklet is considered as positive ($y = 1$) if its first feature, x_0 , corresponds to the same individual than the rest of features of the tracklet, and it is considered as negative ($y = 0$) in the opposite case, as Eq. 2 defines. The identity rendered by the T last features of the tracklet is given by the identity represented by the most of its components (the mode, Mo) since some intruders (with different id) can be added to the tracklet to simulate failed

²The Normalised Double-Margin-based Contrastive Loss function has been implemented in a Caffe python layer, which is publicly available under <http://github.com/magomez/N2M-Contrastive-Loss-Layer>

³The data generation tool, which includes a data balancing method, is composed of a set of C++ functions that are publicly available under http://github.com/magomez/dataset_factory/tree/master/data_factory_from_mot

⁴The C++ class needed to interpret the network architecture and its pre-trained weights is publicly available under https://github.com/magomez/feature_computation

associations.

$$y = \begin{cases} 1 & \text{if } ID(x_0) = Mo(ID(x_n)) \\ 0 & \text{if } ID(x_0) \neq Mo(ID(x_n)) \end{cases} \quad (2)$$

A feature tracklet-based version of the Mini-Batch Gradient Descent algorithm has been implemented to train the presented neural model, and its main procedures, along with the learning iterations, it , are described by Algorithm 1. This algorithm is based on the use of the cross-entropy loss, f_{CE} to compute the loss function, f_L , as Eq.3 and 4 define, on its forward propagation and its derivatives, Eq. 5, on the backward propagation. These partial derivatives are finally used to update the weights using the Adagrad optimisation method, [34].

Algorithm 1 Feature Tracklet-based Mini-Batch Gradient Descent Learning Algorithm.

Require: Batch of feature tracklets, $X^{it} = \{X_i^{it}\}$.

Ensure: The network parameters $W^{IT} = W_j^{IT}$

```

1:  $W^0 = \{w_j^0\}$ 
2: while  $it < IT$  do
3:    $it \leftarrow it + 1$ 
4:    $\frac{\partial f_L}{\partial W_j} = 0$ ;
5:   for all training tracklet  $X_i$  of the batch set  $X^{it}$  do
6:     Calculate  $Z_i = (Z_{i,0}, Z_{i,1})$  by forward propagation;
7:     Calculate  $\sigma(Z_{i,n})$  by Eq. 1;
8:     Calculate  $f_{CE}(W^{it}; X_i^{it})$  by Eq.4;
9:   end for
10:  Calculate  $f_L(W^{it}; X^{it})$  by Eq. 3;
11:  for all training tracklet  $X_i$  of the batch set  $X^{it}$  do
12:    Calculate  $\frac{\partial f_{CE}(W^{it}; X_i^{it})}{\partial W_j^{it}}$ , by back propagation;
13:  end for
14:  Calculate  $\frac{\partial f_L(W^{it}; X^{it})}{\partial W_j^{it}}$  according to Eq. 5;
15:  Update parameters according to Adagrad method;
16: end while

```

$$f_L = \frac{1}{b} \sum_{i=1}^B f_{CE}(W^{it}; X_i^{it}) \quad (3)$$

$$f_{CE}(W^{it}; X_i^{it}) = -y_{i,0} \cdot \log(\sigma(Z_{i,0})) - (1 - y_{i,0}) \cdot \log(1 - \sigma(Z_{i,0})) \quad (4)$$

$$\frac{\partial f_L(W^t; X^t)}{\partial W_j^t} = \frac{1}{B} \sum_{i=1}^B \left[\frac{\partial f_{CE}(W^t; X_i^t)}{\partial W_j^t} \right] \quad (5)$$

5 Tracklets Generation

To create a set of training tracklets, a data creation module has been employed⁵. This tool extracts person images from the MOT17 dataset. However, instead of forming tracklets directly from these images, firstly features are computed from them, and subsequently, the features are used to create the training, validation and test set of tracklets. Each feature, x_n , is computed from a image captured in the frame denoted by $f(x_n)$, and corresponds to the identity $ID(x_n)$.

Five different formulations have been designed to combine the features, and consequently, five different types of tracklets sets, $X_I, X_{II}, X_{III}, X_{IV}, X_V$, have been created and used to train the MS-DoAS network, and the resulting models have been evaluated.

These formulations are defined by the following equations, where M is the set size, that is its number of tracklets. Every set is formed by the random mixture of two subsets, one is formed by positive, X^+ , and the other one, by negative samples, X^- .

⁵The data generation tool has been implemented as a set of C++ functions, which are publicly available under http://github.com/magomez/dataset_factory/tree/master/data_factory_from_mot

The first set, X_I , is the simplest one. Every tracklet is formed by features of a certain person in consecutive frames, as Fig. 3 shows. And in the case of the negative tracklets, a different person representation is taken as component x_0 to simulate the comparison of an agent with a non-corresponding measurement. The subsets of positive and negative samples for the first set, X_I^+ and X_I^- , are defined by Eq. 6 and 7 respectively.



Figure 3: Examples of the images from which tracklets of the set X_I are generated. Positive tracklets are underlined in green, and negatives, in red. f renders the number of the frame from which the first component was extracted, in the sequences of the MOT17 dataset.

$$X_I^+ := X_i = [x_n] \Leftrightarrow \forall n \in Z \cap [0, T-1], f(x_n) - f(x_{n+1}) = 1 \wedge \forall n \in Z \cap [0, T], ID(x_n) = k \wedge i \leq M \quad (6)$$

$$X_I^- := X_i = [x_n] \Leftrightarrow \forall n \in Z \cap [1, T-1], f(x_n) - f(x_{n+1}) = 1 \wedge \forall n \in Z \cap [1, T], ID(x_n) = k \wedge ID(x_0) \neq k \wedge i \leq M \quad (7)$$

The second set, X_{II} , is similar to the previous one. However, in positive tracklets, the frame from which component x_0 is extracted has not to be consecutive to that for component x_1 , but a maximum time step (number frames difference) of F frames is allowed between them. In that way, the identification of a person after a short-term occlusion can be simulated to train the model to re-identify agents. The subsets of positive and negative samples for the second set, X_{II}^+ and X_{II}^- , are defined by Eqs. 8 and 9, respectively.

$$X_{II}^+ := X_i = [x_n] \Leftrightarrow \forall n \in Z \cap [1, T-1], f(x_n) - f(x_{n+1}) = 1 \wedge f(x_0) - f(x_1) < F \wedge \forall n \in Z \cap [0, T], ID(x_n) = k \wedge i \leq M \quad (8)$$

$$X_{II}^- \equiv X_I^- \quad (9)$$

The third set, X_{III} , allows until S time steps with a maximum size of F . Therefore, not only component x_0 can be extracted from non-consecutive frames to the adjacent component, but also other randomly located time steps can be generated in both, positive and negative tracklets. In that way, agents' re-identification in previous frames is simulated. The subsets of positive and negative samples for the third set, X_{III}^+ and X_{III}^- , are defined by Eqs. 10 and 11, respectively.

$$X_{III}^+ := X_i = [x_n] \Leftrightarrow \forall n \in Z \cap [0, T-1], f(x_n) - f(x_{n+1}) \leq F \wedge \forall n \in \{j\}, \{j\} \subset Z \cap [0, T] \wedge |\{j\}| > (T+1-S), f(x_n) - f(x_{n+1}) = 1 \wedge \forall n \in Z \cap [0, T], ID(x_n) = k \wedge i \leq M \quad (10)$$

$$\begin{aligned}
X_{III}^- := X_i = [x_n] &\Leftrightarrow \forall n \in Z \cap [1, T-1], f(x_n) - f(x_{n+1}) \leq F \wedge \forall n \in \{j\}, \\
&\{j\} \subset Z \cap [0, T] \wedge |\{j\}| > (T+1-S), f(x_n) - f(x_{n+1}) = 1 \wedge \forall n \in Z \cap [1, T], \\
&ID(x_n) = k \wedge ID(x_0) \neq k \wedge i \leq M \quad (11)
\end{aligned}$$

The fourth set, X_{IV} , is similar to the first one but until N intruders are added in random locations of the positive and negative tracklets. That means, that some components are substituted by features of different people, to simulate incorrect associations in previous frames. The subsets of positive and negative samples for the fourth set, X_{IV}^+ and X_{IV}^- , are defined by 12 and 13, respectively, where \circ renders the component-wise product operation. In these equations, V_i renders a binary mask vector, of the same length than the tracklets, randomly generated for every tracklet, i . Positions, where the mask takes value 1, corresponds to the introduction of an intruder. X'_i is a tracklet formed by randomly picked intruders. V_i and X'_i are different for every created tracklet.

$$\begin{aligned}
X_{IV}^+ := \{X_i \circ (\neg V_i) + X'_i \circ V_i \mid V \in Z^{T+1} \wedge V_{i,n} \in Z \cap [0, 1] \wedge \sum_{n=0}^T V_{i,n} \leq N \wedge \\
ID(x'_i n) \neq ID(x_0) \wedge X_i \in X_I^+\} \quad (12)
\end{aligned}$$

$$\begin{aligned}
X_{IV}^- := \{X_i \circ (\neg V_i) + X'_i \circ V_i \mid V_i \in Z^{T+1} \wedge V_{i,n} \in Z \cap [0, 1] \wedge \sum_{n=0}^T V_{i,n} \leq N \wedge \\
ID(x'_i n) \neq Mo(ID(x_n)) \wedge X_i \in X_I^-\} \quad (13)
\end{aligned}$$

The fifth set, X_V , is a combination of the third and the fourth set. It includes time steps and intruders, to train the model with a challenging dataset, making it robust to deal with real inputs when it is applied in a tracking algorithm. The subsets of positive and negative samples for the fifth set, X_V^+ and X_V^- , are defined by Eqs.14 and 15, respectively.

$$\begin{aligned}
X_V^+ := \{X_i \circ (\neg V_i) + X'_i \circ V_i \mid V_i \in Z^{T+1} \wedge V_{i,n} \in Z \cap [0, 1] \wedge \sum_{n=0}^T V_{i,n} \leq N \wedge \\
ID(x'_i n) \neq ID(x_0) \wedge X_i \in X_{III}^+\} \quad (14)
\end{aligned}$$

$$\begin{aligned}
X_V^- := \{X_i \circ (\neg V_i) + X'_i \circ V_i \mid V_i \in Z^{T+1} \wedge V_{i,n} \in Z \cap [0, 1] \wedge \sum_{n=0}^T V_{i,n} \leq N \wedge \\
ID(x'_i n) \neq Mo(ID(x_n)) \wedge X_i \in X_{III}^-\} \quad (15)
\end{aligned}$$

It should be noted that in the negative tracklets of training sets IV and V, X_{IV}^- and X_V^- , the component x_0 could present same *id* as some of the intruders, making the discrimination harder.

In order to generate a wide variety of tracklets, the intruder components and the x_0 component in the negative tracklets has been obtaining not only by taking different person detections from the same sequence but also from different ones, resulting in larger and cross-sequence training sets of tracklets.

6 Experimental Results

To evaluate the proposed model, both, its discriminative capacity and the performance of the MOT algorithm where the model has been integrated have been tested. The used dataset and the protocol followed to train and test the model are described below.

6.1 Datasets

The MOT17⁶ dataset has been selected to train and test the model. This dataset belongs to the MOTchallenge⁷ and was released in 2017. It contains fourteen variate real-world surveillance video sequences in unconstrained environments (twelve outdoor

⁶MOT17 dataset is publicly available under <https://motchallenge.net/>

⁷MOTChallenge is a Multiple Object Tracking Benchmark which provides a unified framework to standardise the evaluation of MOT methods. This is published under <https://motchallenge.net/>

sequences and two indoor sequences), filmed with both static and moving cameras. It contains the same sequences as MOT16 [35], but with an extended more accurate ground truth. The resolution is 1920x1080 in twelve of the sequences and 640x480 in the rest of them. There is a total of 11235 frames and 546 different identities.

The sequences of MOT17 dataset are split into two groups. The sequences of the first group are labelled, i.e. they are accompanied by their ground true files with annotations about individuals' location and identity. Person images have been extracted from this group, and they have been divided, in turn, in two groups to train and test the discrimination capacity of the proposed neural model.

Secondly, the unlabelled sequences of the second set have been used to evaluate an MOT algorithm where the proposed MS-DoAS model has been used. Since the ground truth of these sequences is not publicly available, the algorithm's output has been submitted to the public evaluation platform of the MOT Challenge, which provides the results of calculating standard performance metrics.

Furthermore, for every sequence, MOT17 dataset provides the detections given by three different people detectors (DPM[36], Faster-R-CNN [37], and SDP [38]). Therefore, three different versions of every sequence are available, resulting in 42 sequences.

6.2 Evaluation of the discriminative capacity of the model

This article proposes measuring the Degree of Appearance Similarity through a pair-wise binary classification model. This has been evaluated as a binary classifier, in order to test its performance to discriminate between positive and negative tracklets, which is rendered by a ROC curve [39].

This curve illustrates the diagnostic ability of a binary classifier as its discrimination threshold, th , is varied. th defines the value until which the classifier output, MS-DoAS metric, is considered as the prediction of a negative tracklet, and from which it is considered as a positive tracklet. In that way, the chosen threshold, th , divides the distance space in two ranges of values corresponding to each class.

The ROC curve plots the True Positive Rate (TPR) against the False Positive Rate (FPR), defined by Eqs. 16 and 17, respectively, where TP , TN , FP and FN are the number of true positives, true negatives, false positives and false negatives, respectively.

$$TPR = \frac{TP}{TP + FN} \quad (16)$$

$$FPR = \frac{FP}{FP + TN} \quad (17)$$

Moreover, $F1$ score, defined by Eq. 19 provides a trade-off between the Positive Predictive Value, (PPV), Eq. 18, and the True Positive Rate (TPR), Eq. 16. For that reason $F1$ has been used to compare methods in the conducted evaluation, as well as, the Accuracy metric, A , defined by Eq. 20, which is the proportion of well-classified samples. The number of positive and negatives samples in the test set has been completely balanced to provide a fair evaluation through the accuracy metric, which is not appropriate for the case of having skewed classes.

$$PPV = \frac{TP}{TP + FP} \quad (18)$$

$$F1 = \frac{2 \cdot PPV \cdot TPR}{PPV + TPR} \quad (19)$$

$$A = \frac{TP + TN}{TP + FP + TN + FN} \quad (20)$$

Five different formulations have been designed to generate training tracklets that simulate the tracking of the following type of agents:

- I. People who have been previously well identified.
- II. Just re-identified people after a temporary disappearance.
- III. People who have suffered from several disappearances, i.e. their tracks have been interrupted several times.
- IV. People who have been wrongly identified (mismatched) in some of the previous frames.

V. People who have suffered from several disappearances and mismatches.

Five different experiments have been conducted. They are called Exp.MS-DoAS.i, where i takes value 1, 2, 3, 4, or 5 to denote that the model has been trained on the set $TR_1, TR_2, TR_3, TR_4,$ or $TR_5,$ respectively. Every experiment provides a model that has been tested over five different test sets $TS_1, TS_2, TS_3, TS_4, TS_5,$ which were also generated according to the five presented tracklets formulations. Therefore 25 different tests have been performed.

Fig. 4 presents a comparative graphic for every obtained MS-DoAS model. Each graphic shows the ROC curves resulting from testing the query model over the five test sets. On the other hand, Fig. 5 presents a comparative graphic for every test set. Each graphic shows the ROC curves resulting from testing every obtained model over the query test set. Moreover, tables 2 and 3 show the highest values of the $F1$ score and the accuracy metric, $A,$ for each one of the 25 conducted tests. These tables also provide the classification threshold, $th,$ with which the maximum values were achieved.

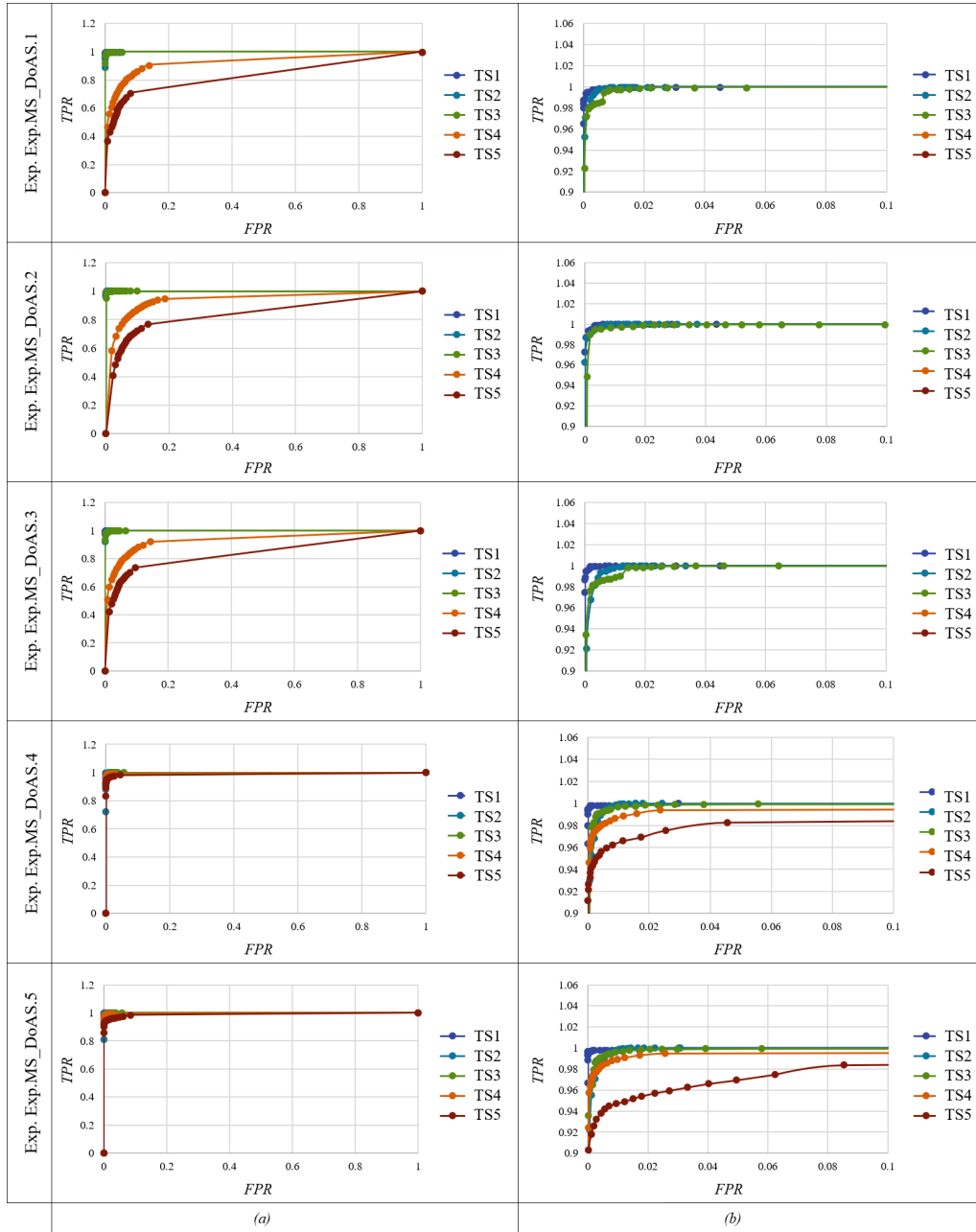


Figure 4: ROC curves from the evaluation of every MS-DoAS model on five different test sets (a), and zoomed region (b).

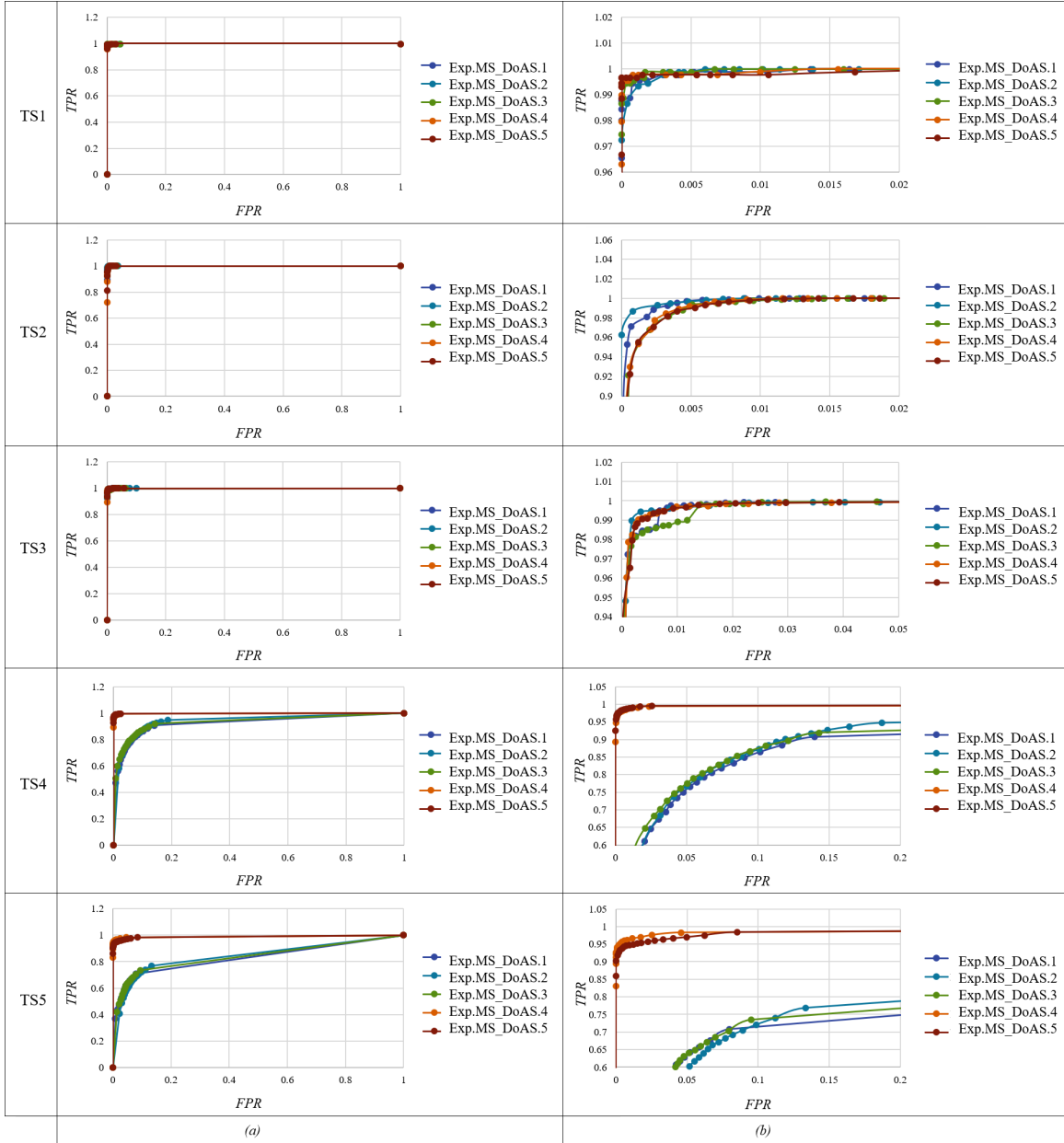


Figure 5: ROC curves from five different evaluations conducted for each one of the MS-DoAS models (a), and zoomed region (b).

Table 2: Maximum $F1$ score value (in [%]) for every MS-DoAS model, evaluated over five different test sets, and th value where it is achieved.

	TS ₁	TS ₂	TS ₃	TS ₄	TS ₅
Exp.MS_DoAS.1	99.74	99.63	99.43	85.37	77.57
	($th=0.45$)	($th=0.45$)	($th=0.55$)	($th=0.9$)	($th=0.95$)
Exp.MS_DoAS.2	99.78	99.6	99.54	86.17	78.24
	($th=0.3$)	($th=0.3$)	($th=0.15$)	($th=0.7$)	($th=0.95$)
Exp.MS_DoAS.3	99.86	99.42	99.19	86.01	78.38
	($th=0.4$)	($th=0.25$)	($th=0.55$)	($th=0.85$)	($th=0.95$)
Exp.MS_DoAS.4	99.85	99.49	99.39	98.66	97.49
	($th=0.5$)	($th=0.65$)	($th=0.45$)	($th=0.65$)	($th=0.75$)
Exp.MS_DoAS.5	99.84	99.43	99.39	98.8	96.65
	($th=0.35$)	($th=0.5$)	($th=0.45$)	($th=0.65$)	($th=0.4$)

Table 3: Maximum Accuracy, A , value (in [%]) for every MS-DoAS model, evaluated over five different test sets, and th value where it is achieved.

	TS ₁	TS ₂	TS ₃	TS ₄	TS ₅
Exp.MS_DoAS.1	99.74	99.63	99.43	88.56	83.43
	($th=0.45$)	($th=0.45$)	($th=0.55$)	($th=0.8$)	($th=0.95$)
Exp.MS_DoAS.2	99.78	99.60	99.54	88.92	82.83
	($th=0.3$)	($th=0.3$)	($th=0.15$)	($th=0.4$)	($th=0.85$)
Exp.MS_DoAS.3	99.86	99.42	99.19	89.09	83.59
	($th=0.4$)	($th=0.25$)	($th=0.55$)	($th=0.75$)	($th=0.95$)
Exp.MS_DoAS.4	99.85	99.49	99.39	98.97	98.00
	($th=0.5$)	($th=0.65$)	($th=0.45$)	($th=0.65$)	($th=0.75$)
Exp.MS_DoAS.5	99.84	99.43	99.39	98.08	97.35
	($th=0.35$)	($th=0.50$)	($th=0.45$)	($th=0.65$)	($th=0.4$)

In general, the classification tests prove the high capacity of the proposed model to discriminate between positive and negative tracklets.

The tests performed over the test sets from TS₁ to TS₅ are progressively harder since the tracklets on these tests simulate increasingly challenging situations. For that reason, the results are worse from TS₁ to TS₅. The models obtained from Exp.MS_DoAS.4 and 5 provide good results for TS₅, so they are capable to deal with real tracking situations.

The models learnt utilizing the training sets from TR₁ to TR₅ are capable of managing progressively more difficult situations, but in detriment of the performance to deal with the easiest identifications. Therefore, a trade-off solution must be chosen, which is given by the models learnt through Exp.MS_DoAS.4 and Exp.MS_DoAS.5.

Before developing the proposed Multi-Shot DoAS model, a Single-Shot version was also trained, where the input was not a tracklet, but a pair of images. This model also employed a previously trained VGG11 neural network to compute the features of the input images. Subsequently, the features were compared by the Euclidean distance. This model achieved an accuracy value of 91.7% and a $F1$ score of 91.9%, which are considerably good values for a challenging task as appearance identification in a MOT sequence.

Nevertheless, the performance of this metric has been overcome by the novel MS-DoAS model, thanks to the incorporation of temporary consistency with a Multi-Shot design.

6.3 Evaluation of the Multi-Object Tracking performance

A tracking-by-detection algorithm has been implemented, where data association is mainly performed by measuring the MS-DoAS between the people detected at every new frame, and the previously tracked identities. The MS-DoAS model has been trained to deal with complex person identification to obtain robust tracking in variate real-world scenarios.

The MOT performance of the proposed algorithm has been quantitatively measured over the test sequences of MOT17 by the MOTA (Multi-Object Tracking Accuracy). Its computation combines three error sources: false positives, missed targets and identity switches, as Eq. 21 describes, where \overline{FN} , \overline{FP} and \overline{IDsw} sum the number of false negatives, FN_f , false positives,

FP_f , and identification switches, $IDsw_f$, in Eqs. 22, 23 and 24 respectively, at every frame, f , of the dataset. All them are divided by the sum of the number of ground truth objects, g_f , at every frame.

$$MOTA = 1 - (\overline{FN} + \overline{FP} + \overline{IDsw}) \quad (21)$$

$$\overline{FN} = \frac{\sum_f FN_f}{\sum_f g_f} \quad (22)$$

$$\overline{FP} = \frac{\sum_f FP_f}{\sum_f g_f} \quad (23)$$

$$\overline{IDsw} = \frac{\sum_f IDsw_f}{\sum_f g_f} \quad (24)$$

Other metrics to measure the MOT performance are:

- *IDF1* Score [40], which is the ratio of correctly identified detections over the average number of ground-truth and computed detections.
- *MT*, Mostly tracked targets. This is the ratio of ground-truth trajectories that are covered by a track hypothesis for at least 80% of their respective life span.
- *ML*, Mostly lost targets. This is the ratio of ground-truth trajectories that are covered by a track hypothesis for at most 20% of their respective life span.

Table 4 shows the obtained scores for the tracking metrics described above. This table lists the results for every sequence as well as the global results (marked in bold). The columns corresponding to metrics for which higher scores mean better performance, present white background, and those for which lower scores mean better performance are shaded.

Table 4: Multi-Object Tracking performance of algorithm MOT.2 over MOT17 dataset. *MOTA*, *FP*, *FN*, *IDsw*, *IDF1*, *MT* and *ML* values.

Sequence	<i>MOTA</i>	<i>FP</i>	<i>FN</i>	<i>IDsw</i>	<i>IDF1</i>	<i>MT</i>	<i>ML</i>
MOT17-01-DPM	23.2%	414	4, 465	74	33.2%	8.3%	41.7%
MOT17-03-DPM	41.7%	6, 280	54, 121	595	45.9%	10.1%	25.0%
MOT17-06-DPM	39.1%	175	6, 891	112	43.8%	5.9%	57.2%
MOT17-07-DPM	30.5%	263	11, 356	115	39.1%	1.7%	48.3%
MOT17-08-DPM	16.7%	592	16, 889	116	23.2%	0.0%	59.2%
MOT17-12-DPM	26.7%	711	5, 576	69	42.8%	2.2%	50.5%
MOT17-14-DPM	17.5%	866	14, 238	143	29.8%	1.8%	62.8%
MOT17-01-FRCNN	24.9%	1, 238	3, 563	41	41.0%	20.8%	33.3%
MOT17-03-FRCNN	54.9%	1, 487	45, 466	249	55.4%	22.3%	18.9%
MOT17-06-FRCNN	47.1%	330	5, 808	99	49.6%	10.4%	38.7%
MOT17-07-FRCNN	29.5%	770	10, 979	153	37.9%	3.3%	38.3%
MOT17-08-FRCNN	18.6%	576	16, 527	97	24.3%	2.6%	57.9%
MOT17-12-FRCNN	34.2%	332	5, 344	23	48.5%	9.9%	57.1%
MOT17-14-FRCNN	18.4%	1, 535	13, 321	221	30.7%	3.0%	56.1%
MOT17-01-SDP	36.0%	692	3, 321	118	38.6%	25.0%	29.2%
MOT17-03-SDP	64.6%	2, 312	34, 207	587	59.7%	31.8%	14.2%
MOT17-06-SDP	49.0%	361	5, 527	117	48.5%	12.6%	40.5%
MOT17-07-SDP	37.7%	475	9, 838	217	44.5%	6.7%	36.7%
MOT17-08-SDP	23.2%	194	15, 880	159	27.1%	5.3%	53.9%
MOT17-12-SDP	35.3%	371	5, 187	48	45.3%	8.8%	53.8%
MOT17-14-SDP	26.3%	1, 061	12, 293	263	36.0%	1.8%	48.2%
Global	42.3%	21, 035	300, 797	3, 616	46.8%	9.1%	44.1%

In addition, the global identification precision P , takes value 69.9% and the global recall, R , 35.2%.

More than ninety algorithms participate in the MOT17 challenge with *MOTA* values from 54.7% to -7.3% . Therefore, the proposed MOT₂, whose *MOTA* value is 42.3%, can be considered as a relatively effective and robust algorithm. Moreover, it is necessary to highlight the fact that the same algorithm, with the same hyper-parameters setting, has been evaluated over all the MOT17 sequences, proving that the presented method is versatile under multiple and variate tracking situations.

Besides, the proposed model allows a frame-by-frame data association, resulting in an online tracking algorithm, i.e. the solution is immediately available with each incoming frame and is not changed at any later time, so that, this approach enables real-time surveillance. Conversely, the top algorithms from the challenge, LSST17 [41] and DGCT, are based on offline (non-causal) methods that rely on future observations.

This article presents the designing of a novel contrastive metric, the MS-DoAS. However, the performance of the tracking algorithm depends on all the involved stages: detection, agents' state prediction, data association method, and the used contrastive metric. Promising results have been obtained by uniquely addressing this last part, so the complete MOT algorithm is susceptible to potential enhancements.

7 Conclusions

This article presents a novel contrastive Deep Convolutional Neural model to perform Multi-Shot recognition by measuring the Degree of Appearance Similarity, MS-DoAS, between successive detections in a Multi-Object Tracking algorithm.

The design of a Multi-Shot architecture provides temporary consistency to the appearance model, whose recognition capacity is higher than that of its Single-Shot version.

Moreover, the proposed model has been trained to deal with different challenging situations, such as with failed associations from previous frames and crossing agents, preventing from further propagation of the identities mismatches. This has been achieved by simulating that type of situations through the training data. The formulation for five tracklets generation mechanisms has been designed and implemented in a software tool that has been publicly delivered.

Eventually, the MS-DoAS model is able to classify quite challenging tracklets with an excellent performance, which makes it suitable for visually identifying a person in a tracking algorithm. Indeed, the tracking of multiple people by a unique visual appearance model without previous knowledge about the scene has been achieved by integrating the proposed model into a plain Tracking-by-Detection algorithm. Its core is a data association mechanism based on taking the MS-DoAS metric as a matching score between two observations.

Besides, the tracking method does not depend on future observations, i.e. it is an online tracking algorithm, and temporary consistency is provided by modelling the agents' appearance with a Long Short-Term Memory neuron.

The designed identification model has been tested over datasets presenting a wide variety and number of people, in outdoors and indoors scenarios, and from fixed and moving cameras, from different perspectives, proving its versatility and robustness against multiple scenarios, and its potential application in upcoming more sophisticated systems.

8 Acknowledgements

Research supported by the Spanish Government through the CICYT projects (TRA2016-78886-C3-1-R and RTI2018-096036-B-C21), Universidad Carlos III of Madrid through (PEVAUTO-CM-UC3M) and the Comunidad de Madrid through SEGVAUTO-4.0-CM (P2018/EMT-4362). We gratefully acknowledge the support of NVIDIA Corporation with the donation of the GPUs used for this research.

References

- [1] Niall McLaughlin, Jesus Martinez Del Rincon, and Paul Miller. Enhancing linear programming with motion modeling for multi-target tracking. In *Applications of Computer Vision (WACV), 2015 IEEE Winter Conference on*, pages 71–77. IEEE, 2015.
- [2] Min Yang and Yunde Jia. Temporal dynamic appearance modeling for online multi-person tracking. *Computer Vision and Image Understanding*, 153:16–28, 2016.
- [3] Keni Bernardin and Rainer Stiefelhagen. Evaluating multiple object tracking performance: the clear mot metrics. *EURASIP Journal on Image and Video Processing*, 2008(1):1–10, 2008.
- [4] Jingchen Liu, Peter Carr, Robert T Collins, and Yanxi Liu. Tracking sports players with context-conditioned motion models. In *Proceedings of the IEEE Conference on Computer Vision and Pattern Recognition*, pages 1830–1837, 2013.

- [5] Erik Meijering, Oleh Dzyubachyk, Ihor Smal, and Wiggert A van Cappellen. Tracking in cell and developmental biology. In *Seminars in cell & developmental biology*, volume 20, pages 894–902. Elsevier, 2009.
- [6] Andreas Ess, Bastian Leibe, Konrad Schindler, and Luc Van Gool. A mobile vision system for robust multi-person tracking. In *2008 IEEE Conference on Computer Vision and Pattern Recognition*, pages 1–8. IEEE, 2008.
- [7] Andreas Ess, Konrad Schindler, Bastian Leibe, and Luc Van Gool. Improved multi-person tracking with active occlusion handling. In *ICRA Workshop on People Detection and Tracking*, volume 2. Citeseer, 2009.
- [8] Rudolph Emil Kalman. A new approach to linear filtering and prediction problems. *Journal of basic Engineering*, 82(1):35–45, 1960.
- [9] Neil J Gordon, David J Salmond, and Adrian FM Smith. Novel approach to nonlinear/non-gaussian bayesian state estimation. In *IEE Proceedings F (Radar and Signal Processing)*, volume 140, pages 107–113. IET, 1993.
- [10] Seung-Hwan Bae and Kuk-Jin Yoon. Robust online multi-object tracking based on tracklet confidence and online discriminative appearance learning. In *Proceedings of the IEEE conference on computer vision and pattern recognition*, pages 1218–1225, 2014.
- [11] Seung-Hwan Bae and Kuk-Jin Yoon. Robust online multiobject tracking with data association and track management. *IEEE transactions on image processing*, 23(7):2820–2833, 2014.
- [12] Jialue Fan, Wei Xu, Ying Wu, and Yihong Gong. Human tracking using convolutional neural networks. *IEEE Transactions on Neural Networks*, 21(10):1610–1623, 2010.
- [13] Nam Le, Alexander Heili, and Jean-Marc Odobez. Long-term time-sensitive costs for crf-based tracking by detection. In *European Conference on Computer Vision*, pages 43–51. Springer, 2016.
- [14] Siyu Tang, Bjoern Andres, Mykhaylo Andriluka, and Bernt Schiele. Multi-person tracking by multicut and deep matching. In *European Conference on Computer Vision*, pages 100–111. Springer, 2016.
- [15] Xiaojing Chen, Le An, and Bir Bhanu. Multitarget tracking in nonoverlapping cameras using a reference set. *IEEE Sensors Journal*, 15(5):2692–2704, 2015.
- [16] Shu Zhang, Yingying Zhu, and Amit Roy-Chowdhury. Tracking multiple interacting targets in a camera network. *Computer Vision and Image Understanding*, 134:64–73, 2015.
- [17] Hyeonseob Nam and Bohyung Han. Learning multi-domain convolutional neural networks for visual tracking. In *Proceedings of the IEEE Conference on Computer Vision and Pattern Recognition*, pages 4293–4302, 2016.
- [18] Guang Shu, Afshin Dehghan, Omar Oreifej, Emily Hand, and Mubarak Shah. Part-based multiple-person tracking with partial occlusion handling. In *2012 IEEE Conference on Computer Vision and Pattern Recognition*, pages 1815–1821. IEEE, 2012.
- [19] David Held, Sebastian Thrun, and Silvio Savarese. Learning to track at 100 fps with deep regression networks. In *European Conference on Computer Vision*, pages 749–765. Springer, 2016.
- [20] Laura Leal-Taixé, Cristian Canton-Ferrer, and Konrad Schindler. Learning by tracking: Siamese cnn for robust target association. In *Proceedings of the IEEE Conference on Computer Vision and Pattern Recognition Workshops*, pages 33–40, 2016.
- [21] Mengyao Zhai, Lei Chen, Greg Mori, and Mehrsan Javan Roshtkhari. Deep learning of appearance models for online object tracking. In *European Conference on Computer Vision*, pages 681–686. Springer, 2018.
- [22] Chanho Kim, Fuxin Li, Arridhana Ciptadi, and James M Rehg. Multiple hypothesis tracking revisited. In *Proceedings of the IEEE International Conference on Computer Vision*, pages 4696–4704, 2015.
- [23] Donald Reid. An algorithm for tracking multiple targets. *IEEE transactions on Automatic Control*, 24(6):843–854, 1979.
- [24] Samuel Schuster, Paul Vernaza, Wongun Choi, and Manmohan Chandraker. Deep network flow for multi-object tracking. In *Proceedings of the IEEE Conference on Computer Vision and Pattern Recognition*, pages 6951–6960, 2017.
- [25] Horesh Ben Shitrit, Jérôme Berclaz, François Fleuret, and Pascal Fua. Multi-commodity network flow for tracking multiple people. *IEEE transactions on pattern analysis and machine intelligence*, 36(8):1614–1627, 2014.
- [26] Bo Yang and Ram Nevatia. An online learned crf model for multi-target tracking. In *2012 IEEE Conference on Computer Vision and Pattern Recognition*, pages 2034–2041. IEEE, 2012.
- [27] Li Zhang, Yuan Li, and Ramakant Nevatia. Global data association for multi-object tracking using network flows. In *Computer Vision and Pattern Recognition, 2008. CVPR 2008. IEEE Conference on*, pages 1–8. IEEE, 2008.
- [28] Horesh Ben Shitrit, Jerome Berclaz, Francois Fleuret, and Pascal Fua. Tracking multiple people under global appearance constraints. In *2011 International Conference on Computer Vision*, pages 137–144. IEEE, 2011.

- [29] Amir Sadeghian, Alexandre Alahi, and Silvio Savarese. Tracking the untrackable: Learning to track multiple cues with long-term dependencies. In *Proceedings of the IEEE International Conference on Computer Vision*, pages 300–311, 2017.
- [30] Karen Simonyan and Andrew Zisserman. Very deep convolutional networks for large-scale image recognition. 2014.
- [31] Alex Krizhevsky, Ilya Sutskever, and Geoffrey E Hinton. Imagenet classification with deep convolutional neural networks. In *Advances in neural information processing systems*, pages 1097–1105, 2012.
- [32] Mar’ia Jos’e Gómez-Silva, Jos’e Mar’ia Armingol, and Arturo de la Escalera. Deep part features learning by a normalised double-margin-based contrastive loss function for person re-identification. In *In Proceedings of the 12th International Joint Conference on Computer Vision, Imaging and Computer Graphics Theory and Applications (VISIGRAPP 2017) (6: VISAPP)*, pages 277–285, 2017.
- [33] María José Gómez-Silva, José María Armingol, and Arturo de la Escalera. Balancing people re-identification data for deep parts similarity learning. *Journal of Imaging Science and Technology*, 2019.
- [34] John Duchi, Elad Hazan, and Yoram Singer. Adaptive subgradient methods for online learning and stochastic optimization. *Journal of Machine Learning Research*, 12(Jul):2121–2159, 2011.
- [35] Anton Milan, Laura Leal-Taixé, Ian Reid, Stefan Roth, and Konrad Schindler. Motu6: A benchmark for multi-object tracking. *arXiv preprint arXiv:1603.00831*, 2016.
- [36] Pedro F Felzenszwalb, Ross B Girshick, David McAllester, and Deva Ramanan. Object detection with discriminatively trained part-based models. *IEEE transactions on pattern analysis and machine intelligence*, 32(9):1627–1645, 2010.
- [37] Shaoqing Ren, Kaiming He, Ross Girshick, and Jian Sun. Faster r-cnn: Towards real-time object detection with region proposal networks. In *Advances in neural information processing systems*, pages 91–99, 2015.
- [38] Fan Yang, Wongun Choi, and Yuanqing Lin. Exploit all the layers: Fast and accurate cnn object detector with scale dependent pooling and cascaded rejection classifiers. In *Proceedings of the IEEE conference on computer vision and pattern recognition*, pages 2129–2137, 2016.
- [39] James A Hanley and Barbara J McNeil. The meaning and use of the area under a receiver operating characteristic (roc) curve. *Radiology*, 143(1):29–36, 1982.
- [40] Ergys Ristani, Francesco Solera, Roger Zou, Rita Cucchiara, and Carlo Tomasi. Performance measures and a data set for multi-target, multi-camera tracking. In *European Conference on Computer Vision*, pages 17–35. Springer, 2016.
- [41] Weitao Feng, Zhihao Hu, Wei Wu, Junjie Yan, and Wanli Ouyang. Multi-object tracking with multiple cues and switcher-aware classification. *arXiv preprint arXiv:1901.06129*, 2019.